THE ROLE OF THE RHO-ROCK PATHWAY IN THE REGULATION OF MICTURITION

PhD Thesis

Helga Balla PharmD

Semmelweis University Doctoral School

Theoretical and Translational Medicine Division

Supervisor: Zoltán Benyó, MD, DSc

Official reviewers: Norbert Szentandrássy, MD, Ph.D

Márton Keszthelyi, MD, Ph.D

Head of the Complex Examination Committee:

Péter Sótonyi, MD, D.Sc

Members of the Complex Examination Committee:

Tamás Radovits, MD, Ph.D

Charaf Hassan, D.Sc

Budapest

2024

1. Introduction

The urinary bladder (UB) is a highly flexible, hollow smooth muscle organ with two main functions: storage of urine and expulsion. A complex neural control system mediates the integration of these functions. Most importantly, the bladder is under the control of the parasympathetic and the sympathetic nervous system. The sympathetic nervous system plays the predominant role in the physiological regulation of the UB during the filling phase. Sympathetic nerves activate smooth muscle contraction in the urethra and the bladder neck along with the relaxation of the detrusor muscle via α_1 and β_3 adrenoreceptors, respectively.

Under physiological conditions, parasympathetic cholinergic neurotransmission seems to play the dominant role in the regulation of the UB compared to that of the adrenergic mechanisms. The parasympathetic nervous system is the key regulator for the urinary bladder smooth muscle (UBSM) contraction with the aim of urine expulsion at the end of the filling phase. When the volume of urine reaches a critical threshold within the bladder, contractions of UBSM cells will co-occur with the opening of the bladder neck and relaxation of the external urethral sphincter resulting in the expulsion of the urine.

Accordingly, the main neurotransmitter to regulate contraction in the urinary bladder is acetylcholine (ACh), which transmits its effects via muscarinic acetylcholine receptors (mAChRs). The mAChRs

comprise five types. It has been established that all mAChRs are expressed throughout the UB, however, the literature on the expression of mAChR subtypes in the detrusor muscle is rather conflicting. On the other hand, several studies in human, rat, guinea pig and rabbit bladders have ambiguously demonstrated that only M_2 and M_3 receptors are expressed in the detrusor and principally mediate UBSM contractions. Moreover, it has been established, that the contribution of the mAChRs to the regulation of the UBSM may change under pathophysiological conditions related to detrusor overactivity, for instance, overactive bladder syndrome (OAB).

OAB is a common clinical condition with the symptoms of frequency, nocturia and urgency with or without incontinence. It significantly impairs the overall quality of life. Given the crucial role of ACh, antimuscarinic drugs are considered to be the mainstay for the treatment of OAB. However, despite the development of bladder selective agents, adherence to the therapy remains a challenge due to the extensive side-effect profile (e.g. dry mouth, obstipation) worsening patients' tolerability.

Muscarinic receptors belong to the family of G protein-coupled receptors (GPCRs) with seven-transmembrane domains. The two general pathways leading to smooth muscle contraction after GPCR activation have already been reported. The receptor activation leads to elevated IP_3 concentration, Ca^{2+} release finally increasing myosine light chain kinase activity. The other signaling pathway includes the Rho and the Rho-associated coiled-coil-containing protein kinase

(ROCK) inhibiting myosin light chain phosphatase and leading to a sustained contraction. The significance of the Rho-ROCK pathway has also been elucidated in the context of bladder dysfunction.

In light of the above-mentioned considerations, it is of paramount importance to conduct research on muscarinic receptors and their intracellular signaling in the urinary bladder.

2. Objectives

Although ACh plays an essential role in the regulation of micturition and the alterations of cholinergic neurotransmission have been implicated in the pathogenesis of urinary bladder dysfunctions, our knowledge of the signaling pathways involved in ACh-induced detrusor contraction still remains incomplete.

Antimuscarinics are widely used in the management of OAB, yet several adverse effects limit their application and patients' compliance. Moreover, it has been demonstrated that the Rho-ROCK pathway plays a pivotal role in the regulation of detrusor contraction. Thus, we aimed to better understand the signal transduction of mAChRs and the role of the RhoA-ROCK pathway in murine and human UBSM. Our objective was to elucidate which muscarinic receptor(s) mediate the CCh-induced contraction in the mouse UB. Moreover, we wanted to identify the G proteins involved in the intracellular signaling of CCh-induced detrusor contraction. Furthermore, we also aimed to investigate the role of the Rho-ROCK pathway within the downstream signaling of muscarinic receptor

activation and UBSM contraction. Our final goal is to provide a theoretical basis for the development of a more specific medication for OAB with fewer adverse effects.

3. Materials and methods

3.1. Animals

All procedures were carried out according to the guidelines of the Hungarian Law of Animal Protection (28/1998) and were approved by the Government Office of Pest County (Permission number: PEI/001/2709-13/2014).

Urinary bladders were obtained from adult male (90-120 day-old, 30-35 g) wild-type mice (C57BL/6N strain from Charles River Laboratories, Isaszeg, Hungary, referred to as WT) and from animals deficient in the M_2, M_3, M_2/M_3 receptor (M_2-, M_3-, M_2/M_3-KO), or from mice in which the $G\alpha_{q/11}$-protein encoding genes were conditionally inactivated in a smooth muscle-specific manner ($G\alpha_{q/11}$-KO).

Inactivation of $G\alpha_i$ proteins was achieved by intraperitoneal administration of pertussis toxin (PTX) every 24 hours six times. The control (CTRL) animals received vehicle treatment in the same way as PTX-treated ones. The effectiveness of the PTX treatment was monitored in Langendorff-perfused heart preparations. Briefly, the lack of the $G\alpha_i$-mediated heart-rate-reducing effect of ACh verified the inactivation of $G\alpha_i$ proteins.

3.2. Human urinary bladder tissues

All procedures involving human UB tissues have been approved by the Scientific and Research Committee of the Medical Research Council of Hungary (License No.: 21545-2/2019/EKU). Human UB tissues were obtained from patients undergoing open radical cystectomy due to muscle-invasive bladder malignancy after having obtained written patient consent. An expert uro-pathologist provided bladder specimens of the tumor-free of the bladder which was immediately placed into Hank's Balanced Salt Solution and transported to the myograph laboratory.

3.3. Preparation of UBSM strips

After the euthanasia of the mice by carbon dioxide asphyxiation, the UBs were removed and placed into Krebs solution at 37 °C. Under dissection microscope, adipose and connective tissues were removed from the serosal surface. The whole mucosal layer (urothelium + submucosa) was also gently and completely removed in order to prevent the potential release of paracrine factors from the mucosal epithelium or submucosal tissue and to avoid potential tension changes induced by myofibroblasts. The cleaned detrusor muscle was cut into four strips of equal length for myography.

Human urinary bladder specimens were also placed into Krebs solution. Under a dissection microscope, the serosal tissue and the

mucosal layer were removed. The isolated detrusor muscle specimens were cut into equal, approximately 3 × 2 × 1 mm strips for myography.

3.4. Myography, determination of concentration-response curves

Detrusor muscle strips were mounted perpendicularly on two parallel tissue-holding needles of a myograph. Chambers were filled with 6 mL of 37 °C Krebs solution aerated with carbogen. Detrusor muscle contractions were registered under isometric conditions. The emerging contraction force was measured along the longitudinal axis of the samples parallel with the axis of the force transducer.

Every experiment started with a 60-minute resting period while the UB strips were stretched to and stabilized at a resting tension of 5 mN. After the equilibration period, the UBSM was challenged twice with 124 mM K^+-containing Krebs solution to test the viability of the tissues. After several washes with normal Krebs solution, the contractile effects of carbamoylcholine (CCh, 10^{-4}-10^{-8}M) was measured. Some of the strips were incubated with the ROCK inhibitor Y-27632 (1 μM or 10 μM, 20 min) before the administration of the agonist.

Finally, bladder strips were exposed to 124 mM K^+-containing Krebs solution to retest the viability of the detrusor strips at the end of the experiment. CCh-induced contractions were expressed as the

percentage of the contraction induced by 124 mM K^+ (second administration) in the same preparation.

3.5. Quantification of RhoA activation

Mouse UBs were cut into half and the detrusor muscle was prepared as described above. After 60 min of resting, bladder strips were pre-stretched to 5 mN in myograph chambers containing normal Krebs solution. Next, one-half of each bladder was challenged with a single dose of CCh (3×10^{-5} M, which induces submaximal contraction) or its vehicle. At 3 min after the CCh or vehicle administration, the strips were removed and rapidly snap frozen in liquid nitrogen to stop enzyme activity immediately.

Baseline and its paired CCh-activated sample RhoA activity measurements were performed from the two halves of the same urinary bladder. Activated RhoA-GTP was normalized to the total RhoA content.

3.6. Evaluation of gene expression

To determine the expression levels of the different muscarinic receptor subtypes and the ROCK enzyme, RNA was isolated from urinary bladder smooth muscle.

First-strand complementary cDNA was prepared from tissue RNA preparations using RevertAid First Strand cDNA Synthesis kit and Bio-Rad C1000 Touch PCR thermal cycler. Reverse transcription was carried out according to the manufacturer's instructions using the

following temperature cycles: 25 °C for 5 min, 42 °C for 60 min and 70 °C for 5 min. Thereafter, the cDNA was stored at −20 °C until further analysis.

qPCR reactions were performed on CFX Connect Real-Time PCR Detection System) using SsoAdvanced Universal SYBR Green Supermix. Temperature cycles were as follows: 95 °C for 60 s, 95 °C for 10 s and 58 °C for 30 s (40 cycles), followed by a melting curve analysis by heating from 65 °C to 95 °C with a rate of 0.5 °C/s and continuous fluorescence measurement.

3.7. Data analysis and statistics

The CCh-induced detrusor muscle contraction was defined as the peak value of tension developed after the addition of each concentration of CCh.

Raw qPCR data were analyzed using CFX Maestro Software 2.2 software. Data evaluation, statistical analysis and graphs were performed by GraphPad Prism software (v.6.07; GraphPad Software Inc., La Jolla, CA, USA).

The Pfaffl algorithm, also known as the delta–delta CT (ΔΔCT) method, with efficiency correction, was used to calculate the expression of the β-2 microglobulin (B2m), mAChRs M_1, M_2, M_3, M_4, M_5 and Rho-associated coiled-coil-containing protein kinases Rock1 and Rock2 genes. B2m was considered as the housekeeping gene for normalizing gene expression. For B2m, efficiency was 1.13; for M_1: 1.1; for M_2: 0.9; for M_3: 1.05; for M_4: 1.06; for M_5: 0.97; for $ROCK_1$:

1.08; and for $ROCK_2$: 0.99. The minimum information for the publication of quantitative real-time PCR experiments (MIQE) guidelines was followed during the entire qPCR quantification workflow.

All experimental data are presented as means ± SEM and *n* represents the number of cases.

For statistical analysis, the Mann–Whitney test or Kruskal-Wallis test was used and $P < 0.05$ was considered as statistically significant difference. Statistical analysis and graph plotting were performed with GraphPad Prism software (v.6.07; GraphPad Software Inc., La Jolla, CA, USA).

Concentration-response curves were analyzed with nonlinear regression and the calculated E_{max} and EC50 values are presented on the figures as table inserts.

4. Results

4.1. The Rho-ROCK pathway has a major role in the regulation of carbamoylcholine (CCh)-induced smooth muscle contraction in murine and human urinary bladder

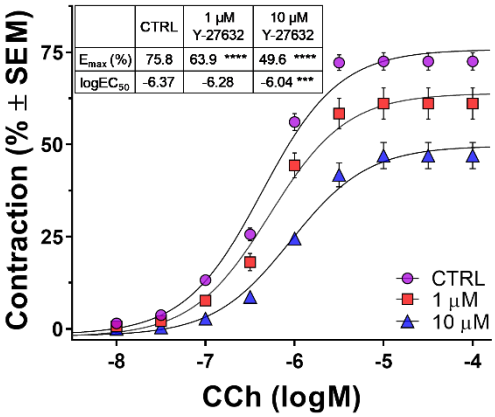

Figure 1 | Role of Rho kinase (ROCK) in mediating carbamoylcholine (CCh)-induced contraction in murine urinary bladder smooth muscle. In mouse detrusor muscle, contractile responses induced by CCh were reduced in the presence of the ROCK inhibitor (Y-27632, 1 and 10 µM). At 1 µM, Y-27632 reduced the E_{max} of the concentration-response curve, whereas there was no statistical difference between the EC_{50} values. However, when Y-27632 was applied at 10 µM, both the EC_{50} and the E_{max} values were statistically different from control (CTRL). CTRL: $n = 14$, 1 µM Y-27632: $n = 12$, 10 µM Y-27632: $n = 8$. ***$P < 0.001$, ****$P < 0.0001$.

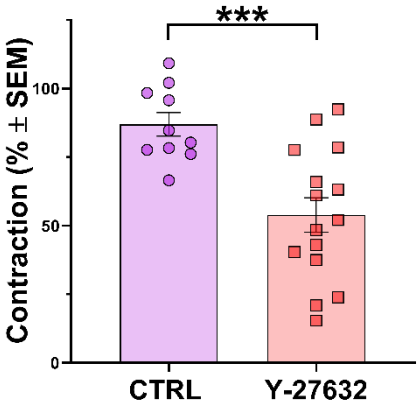

Figure 2 | The ROCK enzyme has a major role in carbamoylcholine (CCh)-induced detrusor contraction in the human urinary bladder. Pretreatment of human urinary bladder smooth muscle strips with the ROCK inhibitor Y-27632 (10 μM, 20 min) reduced contractions induced by CCh (10^{-6} M). CTRL: n = 10, Y-27632: n = 15. Mann-Whitney test, ***$P < 0.001$.

4.2. The role of the M_2 and M_3 receptors in the detrusor muscle contraction and RhoA activation induced by carbamoylcholine (CCh)

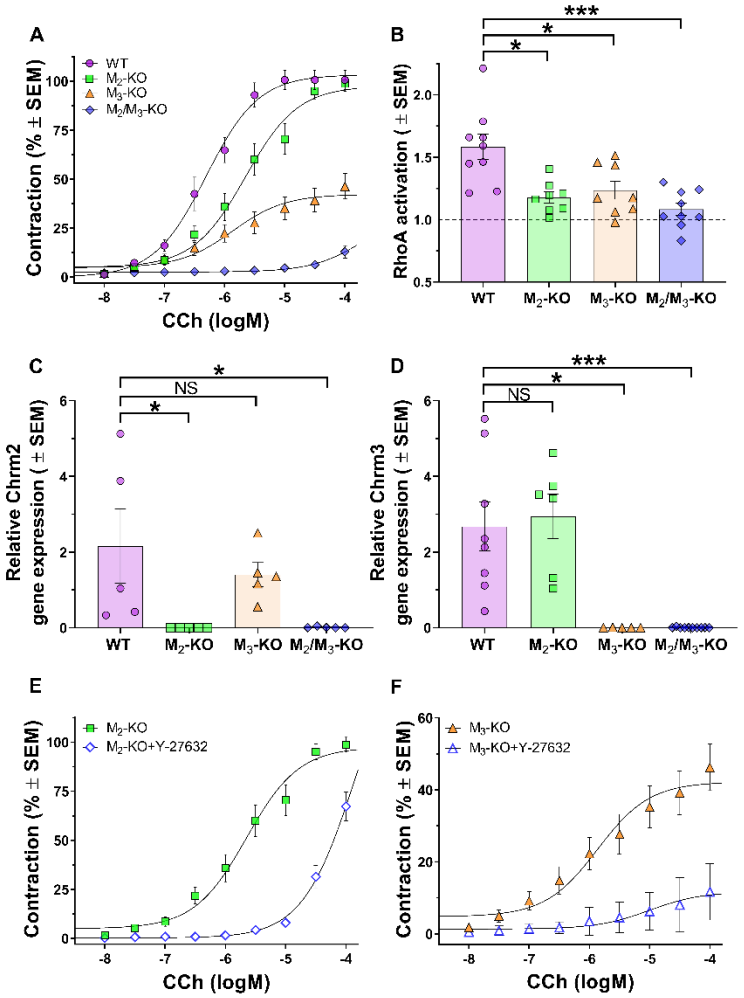

Figure 3 | Carbamoylcholine (CCh)-induced detrusor contraction and RhoA activation are mediated by both M_2 and M_3 muscarinic acetylcholine receptors. A: CCh-induced contractions were markedly impaired in detrusor strips lacking either M_2 (M_2-KO) or M_3 receptors (M_3-KO). Furthermore, the contractile response to CCh was completely abolished in urinary bladder smooth muscle (UBSM) strips deficient in both M_2 and M_3 receptors (M_2/M_3-KO). B: CCh (3×10^{-5} M)-induced RhoA activation significantly decreased in both M_2-KO and M_3-KO mouse bladders and abolished in M_2/M_3-KO UBSM. C: No statistical difference was observed in M_2 receptor gene (*Chrm2*) expression in the M_3 receptor-deficient animals compared to wild type (WT). D: The expression of the M_3 receptor gene (*Chrm3*) was unaffected by the lack of M_2 receptors. E: ROCK inhibitor (Y-27632, 10 μM), induced a further marked decrease in contraction in M_2-KO mouse bladder strips. F: CCh-induced contractions were abolished completely by Y-27632 (10 μM) in UBSM strips deficient in M_3 receptors. A: WT: $n = 6$, M_2-KO: $n = 16$, M_3-KO: $n = 15$, M_2/M_3-KO: $n = 8$, B: WT: $n = 9$, M_2-KO $n = 8$, M_3-KO $n = 8$, M_2/M_3-KO = 9, C: WT: $n = 5$, M_2-KO: $n = 5$, M_3-KO: $n = 5$, M_2/M_3-KO: $n = 5$, D: WT: $n = 8$, M_2-KO: $n = 6$, M_3-KO: $n = 5$, M_2/M_3-KO: $n = 10$, E: M_2-KO $n = 16$, Y-27632: $n = 8$, F: M_3-KO: $n = 6$, Y-27632: $n = 8$. B, C, D: Kruskal-Wallis test, NS not significant, $^*P < 0.05$, $^{***}P < 0.001$.

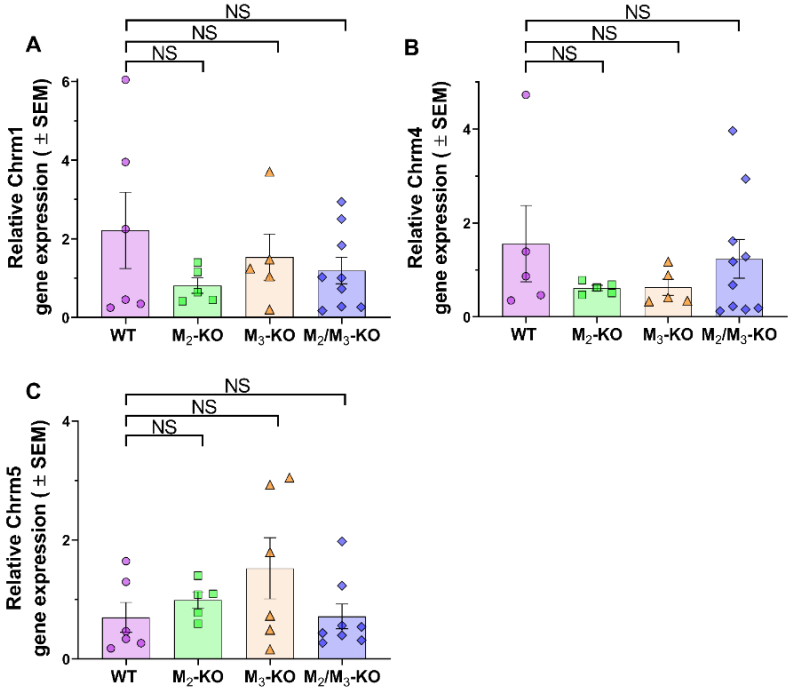

Figure 4 | Expression levels of M_1, M_4, M_5 receptor genes (*Chrm1*, *Chrm4*, *Chrm5*) in detrusor strips from M_2-, M_3-, M_2/M_3-knockout (KO) mice. A: The expression of *Chrm1* was unaffected by the lack of M_2 and M_3 receptors. B: No statistical difference was observed in M_4 receptor gene expression in the receptor-deficient animals compared to wild type (WT). C: The amount of the *Chrm5* did not change in M_2-, M_3- and M_2/M_3-KO mice compared to that of controls. A: WT: $n = 6$, M_2-KO: $n = 5$, M_3-KO: $n = 5$, M_2/M_3-KO: $n = 9$, B: WT: $n = 5$, M_2-KO: $n = 5$, M_3-KO: $n = 5$, M_2/M_3-KO: $n = 10$, C: WT: $n = 6$, M_2-KO: $n = 5$, M_3-KO: $n = 6$, M_2/M_3-KO: $n = 8$. Kruskal-Wallis test, $P < 0.05$ was considered as significant difference.

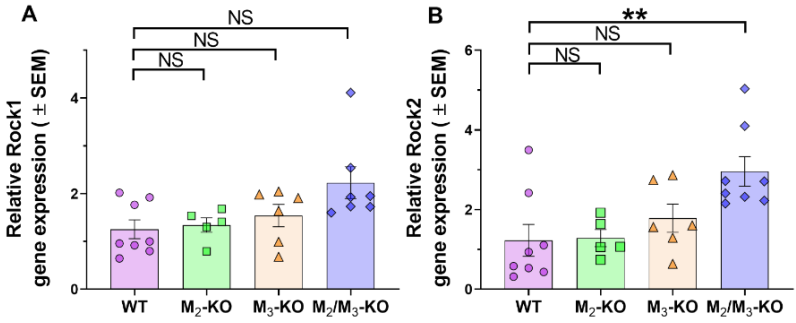

Figure 5 | Gene expression of Rho-associated coiled-coil-containing protein kinase 1 and 2 (*Rock1, Rock2*) in M_2-, M_3- and M_2/M_3- knockout (KO) mice. A: There was no significant difference in the expression of *Rock1* in wild type (WT) and receptor-deficient animals. B: The mRNA expression of the $ROCK_2$ was elevated in M_2/M_3-KO animals compared to that of WT. A: WT: $n = 8$, M_2-KO: $n = 5$, M_3-KO: $n = 6$, M_2/M_3-KO: $n = 7$, B: WT: $n = 8$, M_2-KO: $n = 5$, M_3-KO: $n = 6$, M_2/M_3-KO: $n = 8$. Kruskal-Wallis test, $^{**}P < 0.01$.

4.3. Inhibitory effect of pertussis toxin (PTX) on carbamoylcholine (CCh)-induced urinary bladder smooth muscle contraction and RhoA activation

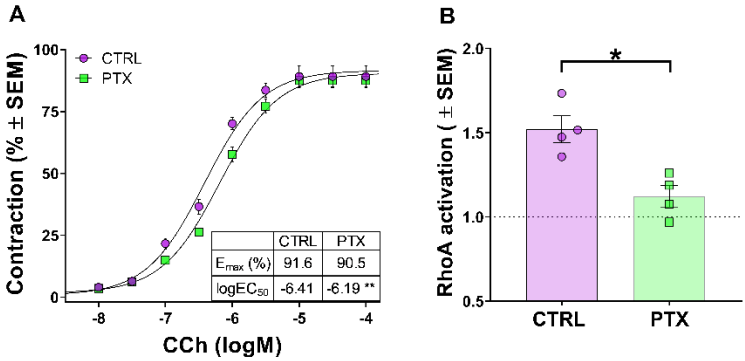

Figure 6 | Inhibition of carbamoylcholine (CCh)-induced detrusor muscle contraction and RhoA activation by pertussis toxin (PTX). A: The concentration-response curve of CCh was shifted to the right in urinary bladder smooth muscle (UBSM) strips from mice treated with PTX without changing the E_{max} value. B: The CCh (3×10^{-5} M)-induced RhoA activation was diminished in UBSM strips from PTX-treated mice. A: CTRL: $n = 19$, PTX: $n = 26$, B: CTRL: $n = 4$, PTX: $n = 4$. $^{**}P < 0.01$. B: Mann-Whitney test, $^{*}P < 0.05$.

4.4. $G\alpha_{q/11}$-coupled signaling pathway plays a key role in urinary bladder contractions but not in RhoA activation induced by carbamoylcholine (CCh)

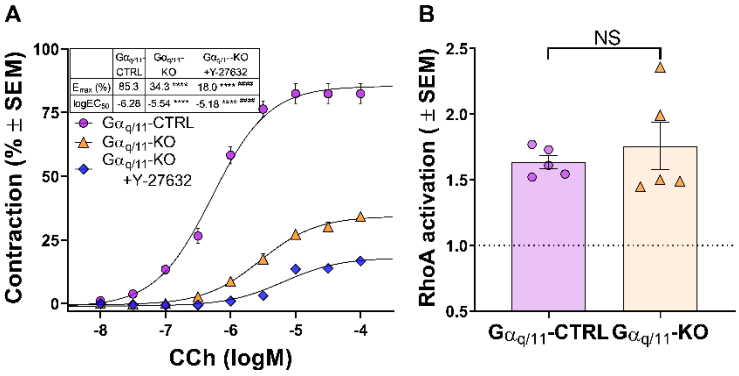

Figure 7 | $G\alpha_{q/11}$ signaling plays a key role in mediating carbamoylcholine (CCh)-induced bladder contractions but not in RhoA activation. A: Detrusor muscle contractions evoked by CCh were markedly decreased in smooth muscle-specific $G\alpha_{q/11}$-knockout (KO) mice and were diminished in the presence of the ROCK inhibitor Y-27632 (10 μM) in the $G\alpha_{q/11}$-deficient animals. B: CCh (3×10^{-5} M)-induced RhoA activation was unaffected by the lack of $G\alpha_{q/11}$ in UBSM. A: $G\alpha_{q/11}$-CTRL: $n = 15$, $G\alpha_{q/11}$-KO: $n = 22$, $G\alpha_{q/11}$-KO + Y-27632: $n = 8$, B: $G\alpha_{q/11}$-CTRL: $n = 5$, $G\alpha_{q/11}$-KO: $n = 5$. Gαq/11-CTRL vs $G\alpha_{q/11}$-KO: ****$P < 0.0001$, $G\alpha_{q/11}$-KO vs $G\alpha_{q/11}$-KO + Y-27632: ####$P < 0.0001$. B: Mann-Whitney test, $P < 0.05$ was considered as significant difference.

5. Conclusion

Since both the storage and voiding phases of the urinary bladder are under complex regulation, even minor alterations can lead to dysfunctions such as involuntary detrusor contraction resulting in detrusor overactivity and the clinical symptoms of OAB. The mAChRs play an unquestionable role in the regulation of micturition and antimuscarinic drugs are mainstays for the treatment of the worldwide symptom complex, OAB. Nevertheless, the exact signaling pathway of mAChRs is obscure even though a more detailed understanding of the signal transduction pathway may help to find more specific drug targets with fewer adverse effects for OAB.

Therefore, in the present study, we aimed to analyze the role of the M_2 and M_3 muscarinic receptors and their corresponding heterotrimeric G proteins (G_i and $G_{q/11}$, respectively) in the regulation of detrusor function, concentrating on the interaction with the Rho-ROCK pathway. We demonstrated that the ROCK plays a pivotal role in the detrusor contraction induced by the muscarinic receptor agonist, CCh. Moreover, the CCh-induced contractions and RhoA activation are mediated by both the M_2 and the M_3 receptors according to the results gained from M_2-, M_3- and M_2/M_3-KO animals. In addition, the expression levels of other muscarinic receptors were not altered by the genetic deletion of M_2 and M_3 receptors indicating that no other muscarinic receptors contribute to the UBSM contraction induced by CCh. Furthermore, pharmacological inhibition of the ROCK enzyme

had an additional inhibitory effect on the concentration-response curve of CCh in M_2- and M_3-KO mice. Interestingly, there was no change in the expression of the $ROCK_1$ enzyme in detrusor muscle from mice deficient in M_2 or M_3 receptors; however, the $ROCK_2$ enzyme expression was elevated in M_2/M_3-KO mice suggesting a compensatory upregulation of ROCK in the absence of both receptors. PTX treatment of WT mice shifted the concentration-response curve of CCh to the right parallel with a steep decrease in RhoA activation. The CCh-induced contractions were diminished in $G_{q/11}$-KO animals however, the RhoA activation did not change in mice deficient in $G_{q/11}$ compared to that of WT. These results indicate that muscarinic receptor-mediated RhoA activation is not mediated by $G_{q/11}$ but rather by G_i.

These observations can support the development of novel, more specific therapeutic targets that can help to improve patient adherence with better-tailored therapeutic strategies of OAB to maximize patients' quality of life and cost-effective care.

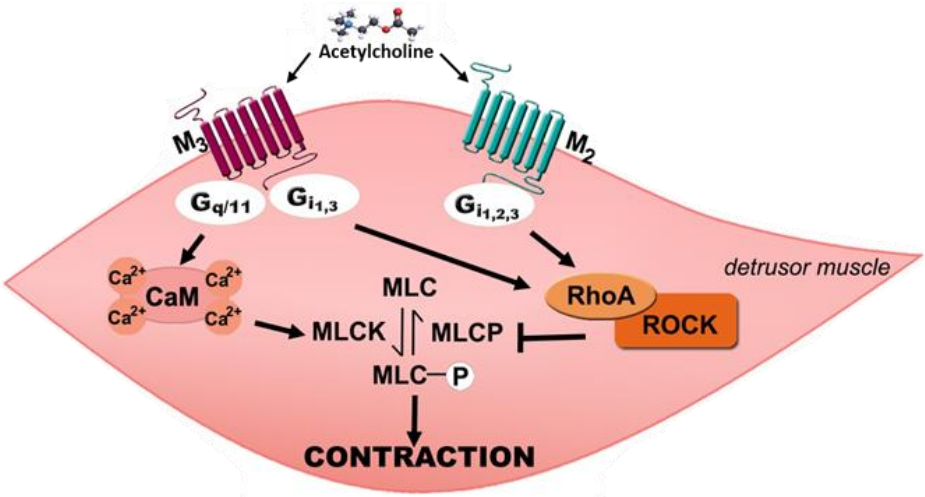

Figure 8 | Proposed model of muscarinic receptor signaling in the murine urinary bladder smooth muscle based on our findings and Offermanns *et al.* (1994). CaM, calmodulin; MLC, myosin light chain; MLCK, myosin light-chain kinase; MLCP, myosin light-chain phosphatase; ROCK, Rho-associated coiled-coil-containing protein kinase.

6. Bibliography of the candidate's publications

Publications related to the dissertation

H. Balla, K. Borsodi, P. Őrsy, B. Horváth, P. J. Molnár, Á. Lénárt, M. Kosztelnik, É. Ruisanchez, J. Wess, S. Offermanns, P. Nyirády, and Z. Benyó, "Intracellular signaling pathways of muscarinic acetylcholine receptor-mediated detrusor muscle contractions", *AMERICAN JOURNAL OF PHYSIOLOGY: RENAL PHYSIOLOGY*, vol. 325, pp. F618–F68, 2023. **IF: 4.200**

K. Borsodi, **H. Balla**, P. J. Molnár, Á. Lénárt, I. Kenessey, A. Horváth, A. Keszthelyi, M. Romics, A. Majoros, P. Nyirády, S. Offermanns, and Z. Benyó, "Signaling Pathways Mediating Bradykinin-Induced Contraction in Murine and Human Detrusor Muscle", *FRONTIERS IN MEDICINE: GERIATRIC MEDICINE*, vol. 8, 2021. **IF: 3.900**

Publications not related to the dissertation

P. J. Molnár, B. Dér, K. Borsodi, **H. Balla**, Z. Borbás, K. Molnár, É. Ruisanchez, I. Kenessey, A. Horváth, A. Keszthelyi, A. Majoros, P. Nyirády, S. Offermanns, and Z. Benyó, "Isoprostanes evoke contraction of the murine and human detrusor muscle via activation of the thromboxane prostanoid TP receptor and Rho kinase",

AMERICAN JOURNAL OF PHYSIOLOGY: RENAL PHYSIOLOGY, vol. 320, no. 4, pp. F537–F547, 2021. **IF: 4.097**

Cumulative impact factor of the candidate's publication: **12.197**